

# Emotion Recognition from EEG Signals using HOS methods: A different approach

Chrysoula Tsimperi, Student Member, IEEE, Pavlos Beltes, Theodoros Katzalis, Leontios Hadjileontiadis, Member, IEEE

**Abstract**—The development of automatic emotion detection systems has gained significant attention due to the growing possibility of their implementation in several applications, including affective computing and various fields within biomedical engineering. Use of the electroencephalograph (EEG) signal is preferred over facial expression, as people cannot control the EEG signal generated by their brain; the EEG ensures a stronger reliability in the psychological signal. However, because of its uniqueness between individuals and its vulnerability to noise, use of EEG signals can be rather complicated. In this paper, we propose a methodology to conduct EEG-based emotion recognition by using High Order Statistics. Specifically, we explore derived features of bispectrum for quantification of emotions using a Valence-Arousal emotion model. These features explore mainly statistical entities applied on the magnitude of the bispectrum and the corresponding behaviour of the coupling pattern of frequencies and peaks. A preliminary cepstral analysis has been also conducted using cepstrum and bicepstrum, showing the potential for further investigation. The results of the bispectrum matrix analysis indicate that the effort of finding distinguished factors for emotion classification focusing per channel and per feature isn't enough to decouple the hidden pattern of emotion recognition. A multi-feature, multi-channel approach would probably be a more beneficial approach.

**Index Terms**—bispectrum, cepstrum, EEG, emotion recognition

## I. INTRODUCTION

EMOTION is a subjective experience characterized by psycho-physiological expressions, biological reactions, and mental states. From a psychological point of view, an emotion is a complex psychological state that involves three distinct components: a subjective experience, a physiological response, and a behavioral or expressive response (Hockenbury and Hockenbury, 2007). Emotion, as a common mental phenomenon, is closely related to our daily life. Although it is easy to sense other people's emotion in human-human interaction, it is still difficult for machines to understand the complicated emotions of human beings. As the first step to make machines capture human emotions, emotion recognition has received substantial attention from human-machine-interaction (HMI) and pattern recognition research communities in recent years. Human emotional expressions are mostly based on verbal behavior methods (e.g. speech), and nonverbal behavior methods (e.g. facial expression). Thus, a

large body of literature concentrates on learning the emotional components from speech and facial expression data. However, from the viewpoint of neuroscience, humans emotion originates from a variety of brain cortex regions, such as the orbital frontal cortex, ventral medial prefrontal cortex, and amygdala, which provides us a potential approach to decode emotion by recording the continuous human brain activity signals over these brain regions. For example, by placing the EEG electrodes on the scalp, we can record the neural activities in the brain, which can be used to recognize human emotions. EEG signals have been proved to have a strong relationship with emotional states. It has higher classification accuracy for emotion recognition by analyzing EEG signals and reacts faster to the emotion changes. Therefore, analyzing EEG signals is more reliable and effective for emotion recognition. Our analysis is roughly based on the process of the EEG-based emotion classification. First of all, we introduce the commonly emotional evocation experiments and EEG datasets for emotion recognition. Secondly, the EEG signals acquisition equipment and electrode distribution in different experimental studies are carried out. After the comparison, the EEG feature analysis methods commonly used in current studies are explained. Finally, we explore derived features of bispectrum for quantification of emotions using a Valence-Arousal emotion model.

## II. DATASETS

In this study, we utilize 2 publicly available dataset for emotion analysis using EEG signals (DEAP and SEED).

### A. DEAP Dataset

[1] DEAP is a multi-modal dataset that comprises EEG and peripheral physiological signals recorded for 32 subjects, including 16 females and 16 males, while watching a set of 40 one-minute video stimuli. The content of each video stimulus was selected to evoke a specific emotional state. For each subject, the recorded EEG signals associated with each video stimulus represent a single trial. The total number of trials within the DEAP dataset is 1280 trials (40 trials per subject), and the length of each trial is 63 s. In particular, each trial starts with a three-second baseline period followed by 60 s of EEG signal recording that corresponds to the subject's response with respect to a specific video stimulus. After each trial, each subject was asked to quantify his/her emotional response with respect to the displayed video in terms of five

The authors are with the Signal Processing and Biomedical Technology Unit, Telecommunications Laboratory, Department of Electrical and Computer Engineering, Aristotle University of Thessaloniki, GR 54124 Thessaloniki, Greece (e-mail: tsimper@ece.auth.gr; mpeltesp@ece.auth.gr; katzalis@ece.auth.gr; leontios@auth.gr)

emotion description scales, namely valence, arousal, dominance, like/dislike and familiarity scales. The values of the valence, arousal, dominance and like/dislike scales are in the range 1-9, while the values of the familiarity scale are in the range 1-5. DEAP database uses carefully-chosen emotional stimuli based on statistical methods from the respondents. To ensure objectivity, the respondents who assessed the emotional stimuli were different from the respondents who recorded the EEG signals. Second, this database provides numerous observations. Using a publicly open database enables us to reproduce and compare our research results with other findings. DEAP database provided the most EEG data from participants; emotional stimuli came from video music clips, and the emotional states of the participants were defined in 2D emotion models (i.e., the arousal and the valence levels), producing four quadrants of emotion: the high arousal, high valence (HAHV); the low arousal, high valence (LAHV); the low arousal, low valence (LALV); and the high arousal, low valence (HALV) emotion classes (Fig. 1).

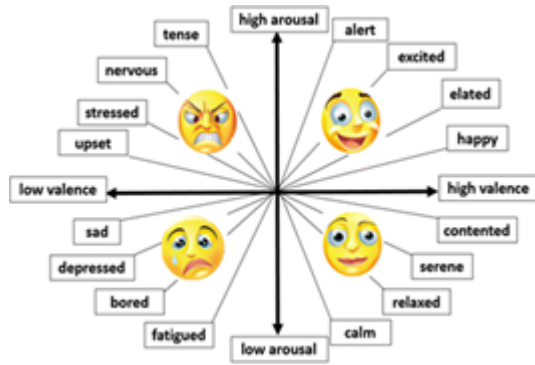


Fig. 1: Arousal-valence plane and label distribution for DEAP dataset

### B. SEED Dataset

The emotion recognition task is carried on SEED [2] dataset developed by SJTU. The EEG dataset was collected by Prof. Bao Liang Lu at brain-like computing and machine Intelligence (BCMI) laboratory. This publicly available dataset contains multiple physiological signals with emotion evaluation, which makes it a well-formed multi-modal dataset for emotion recognition. In this data set, 15 participants were subjected to watch four minutes of six video clips. Each clip is well-edited that can be understood without explanation and exhibits the maximum emotional meanings. The data was collected from 15 Chinese participants (7 males, 8 females), who were aged between 22-24. Each participant's data includes 15 trials, and, in each trial, the experiment performed twice. The raw EEG signals were first segmented and then downsampled to 200 Hz. A bandpass frequency filter of 0-75 Hz was also applied to remove noise from the signal and EMG signals. The data was collected from 62 channels of each participant using 10-20 International standard (Fig. 2).

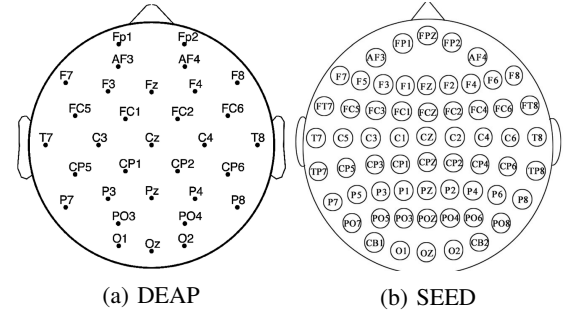


Fig. 2: Electrodes position

## III. METHODS

### A. Signal Decomposition

In this work, a cascaded filtering technique is used to implement the DWT. The signals are decomposed into rhythms with a pair high-pass filter and low-pass filter. It decomposes the signal into the approximation coefficients and detail coefficients of sub-bands. The approximation coefficients are further divided into new approximation and detail coefficients. This process is carried out to the defined level of decomposition [3], [4]. As such there is no wavelet selection criterion that is used for simulation. The selection of the wavelet basis has been done based on literature study [5].

The mother wavelet function  $\Psi_{a,b}(t)$  is given by:

$$\Psi_{a,b}(t) = \frac{1}{a} \Psi\left(\frac{t-b}{a}\right) \quad (1)$$

where  $a = 2^j$  is the scale parameter and  $b = k$ .  $2^j$  is the shift parameter, and both  $j$  and  $k$  are integers. There are mainly five rhythms that are present in the EEG signals at different frequency bands. The frequency ranges covered by various rhythms are categorized as delta (0.1-4Hz), theta (4-8Hz), alpha (8-13Hz), beta (13-30Hz), and gamma (36-40Hz). Fig. 1 depicts the various rhythms present in the considered four-labeled EEG signals of DEAP-dataset. The size of analysis labeled EEG dataset is the order of (number of volunteers (32) × number of channels (40) × number of rhythms (5) × data length (3840)) when last 30-s duration is considered. It is observed that small frequencies are also present in the EEG signals of DEAP-dataset that may arise due to the leakage of filter response. The presence of these small frequencies are also depicted as delta rhythm in Fig. 3.

### B. High Order Statistics

The first and second order statistics (e.g., mean, variance, autocorrelation, power spectrum) are popular signal processing tools and have been used extensively for analysis of process data. But such second order statistics are only sufficient for describing linear and Gaussian processes. In practice, there are many situations when the process deviates from Gaussianity and linearity, e.g., when it exhibits nonlinear behavior. These type of processes can conveniently be studied using Higher Order Statistics (HOS). There are three main reasons for using HOS: to extract information due to deviations from Gaussianity, to recover the true phase character of the signals,

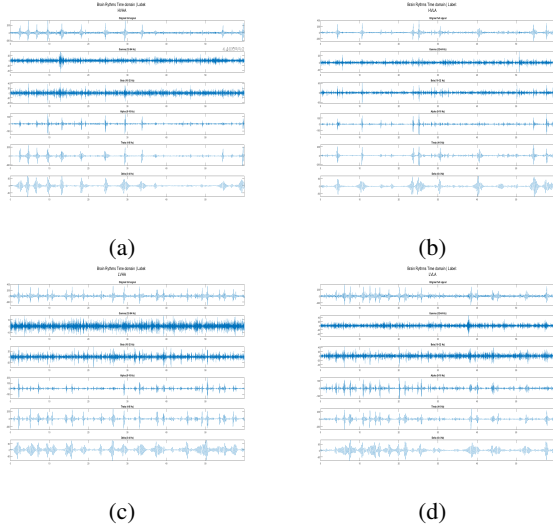


Fig. 3: DEAP-dataset emotion labels Rhythms (gamma, beta, alpha, theta, and delta): (a) HVHA, (b) HVLA, (c) LVHA, and (d) LVLA

and to detect and quantify nonlinearities in time series (Nikias and Petropulu, 1993). The following sections briefly describe some of the HOS terms.

HOS has been claimed as an effective method for analyzing EEG signals. HOS feature has been the most commonly used nonlinear feature. It is the frequency domain or spectral representation of higher order cumulants of a random process. HOS only includes cumulants with third order and above. HOS gains its advantage with the elimination of Gaussian noise and provides a high signal to noise ratio (SNR) [6], [7]. HOS provides the ability to extract information deviation from Gaussian and preserves the phase information of signals. Thus, HOS is able to estimate the phase of the non-Gaussian parametric signals. In addition, HOS detects and characterizes nonlinearities in signals. In contrast, the second order measure is power spectrum, which can only reveal linear and Gaussian information of signals.

The 2D Fourier transform of third order cumulants is the bispectrum and is able to preserve phase information of EEG signals. Bispectrum is the easiest HOS entity to be worked out [8].

The studied signals are having highly nonlinear and non-stationary behavior. The third order coefficients (ToC) is the triple correlation of a signal. It is the function of two lag parameters along with its harmonics that illustrate the presence of non-linearity present in the non-stationary brain signals. It characterized the time-varying information into higher dimensional space that not only preserves the original signal information, but also consists of the harmonics information at higher dimension, and this may better reveal the dynamics of the nervous system. The higher order statistics (HOS) has been used in various biomedical signal processing applications [9], [10], [11], [12]. It gives a nonlinear algorithm that allows analysis of signal in higher dimensional space. The HOS has some unique properties that help to analyze the non-Gaussian signals as given below [13], [14] : a. The ToC

is equal to zero for symmetric distributed random variable, i.e.,  $C_x^k[l_1, l_2, \dots, l_{k-1}] = 0$ . This makes it efficient to analyze the non-Gaussian distributed signal in the presence of Gaussian distributed signals such as noise. b. The Bispectrum is infinitely differentiable and convex that allows analyzing the non-minimum phase and phase coupled signals. It can recognize Gaussian/non-Gaussian signals, linear/nonlinear systems, phase coupling, and more.

### C. Bispectrum and Bicoherence

Bispectrum has been utilized in the emotional study in EEG signals. Not all the information content of a signal may be easily obtained from statistical analysis of the data in the time domain. Transforming the signal from time to frequency domain can expose the periodicities of the signal and can also aid in understanding the signal generating process. Just as the power spectrum is the frequency domain representation of the second order moment, the bispectrum is the frequency domain counterpart of the third order cumulants. However, the emotional states are yet to be analyzed using the bispectrum features. Hence, in this work, the bispectrum feature is used to classify EEG signals in different emotional states. Bispectrum is proven in its ability to detect quadratic phase coupling (QPC), a phenomenon of nonlinearity interaction in EEG signals. QPC is the sum of phases at two frequency variables given by  $f_1 + f_2$  [15], [16]. Bispectrum can be estimated through two approaches: direct and indirect methods. For a stationary, discrete time, random process  $x(k)$ , the direct method is estimated by taking the 1D-Fourier transform of the discrete series given by:

$$B_i(f_1, f_2) = E[X(f_1)X(f_2)X^*(f_1 + f_2)] \quad (2)$$

where  $B_i$  is the bispectrum magnitude,  $E[\cdot]$  denotes statistical expectation operation and  $X(f)$  is the Fourier transform (1-D FFT) of the time series. The bispectrum can be plotted against two independent frequency variables,  $f_1$  and  $f_2$  in a three dimensional plot. Each point in the plot represents the bispectral content of the signal at the bifrequency,  $(f_1, f_2)$ . In fact, the bispectrum at point  $(B(f_1, f_2), f_1, f_2)$  measures the interaction between frequencies  $f_1$  and  $f_2$ . This interaction between frequencies can be related to the non-linearities present in the signal generating systems and therein lies the core of its usefulness in the detection and diagnosis of non-linearities. It can be shown that the bispectral estimates are asymptotically unbiased and the variance of the estimator depends on the second order spectral properties (Hinich, 1982). That is,

$$\text{var}(\hat{B}(f_1, f_2)) \propto P(f_1)P(f_2)P(f_1 + f_2) \quad (3)$$

where,  $P(f)$  is the power of the signal at frequency,  $f$ .

For the indirect method, bispectrum is estimated by first estimating the third order cumulants of the random process  $x(k)$ . Then the  $n^{\text{th}}$ -order moment is equal to the expectation over the process multiplied by the  $(n - 1)$  lagged version of itself. Therefore, the third order moment,  $m_{3x}$  is:

$$m_{3x}(\tau_1, \tau_2) = E[X(k)X(k + \tau_1)X(k + \tau_2)] \quad (4)$$

where  $E[\cdot]$  denotes statistical expectation operation,  $\tau_1$  and  $\tau_2$  are lags of the moment sequence.

The third order cumulant sequence,  $c_3(\tau_1, \tau_2)$ , is identical to its third order moment sequence for zero mean. It can be calculated by taking an expectation over the process multiplied by 2 lagged versions given by:

$$c_3^x = m_3^x(\tau_1, \tau_2) - \cancel{m_1^x} \left[ \cancel{m_2^x}(\tau_1) + m_2^x(\tau_2) + m_2^x(\tau_1 - \tau_2) \right] + 2(\cancel{m_1^x})^3 = m_{3x}(\tau_1, \tau_2) \quad (5)$$

Alternatively to (2), the bispectrum,  $B(f_1, f_2)$ , is the 2D-Fourier transform of the third order cumulant function and is given by:

$$B(f_1, f_2) = \sum_{\tau_1=-\infty}^{\infty} \sum_{\tau_2=-\infty}^{\infty} C_{3x}(\tau_1, \tau_2) \exp[-j(f_1\tau_1 + f_2\tau_2)] \quad (6)$$

for  $|f_1| \leq \pi$ ,  $|f_2| \leq \pi$  and  $|f_1 + f_2| \leq \pi$ .

Since the estimate depends directly on the bifrequency, the variance of the estimate will be higher at a bifrequency where the signal energy is high and will be lower where the energy is low. This causes serious problems in its estimation. Thus, the bispectrum is usually normalized in a such way that it gives a measure whose variance is independent of the signal energy. This is termed as bicoherence and is defined by the following equation

$$bic^2(f_1, f_2) \triangleq \frac{|E[B(f_1, f_2)]|^2}{E[|X(f_1)X(f_2)|^2]E[|X(f_1 + f_2)|^2]} \quad (7)$$

where "bic" is known as the bicoherence function.

It has been shown by (Kim and Powers, 1979) that the variance of the bicoherence estimator satisfies the following expression:

$$\text{var}[\hat{bic}^2(f_1, f_2)] \approx \frac{1}{M} [1 - bic^2(f_1, f_2)] \quad (8)$$

where  $M$  is defined as the number of segments used in the estimation. A useful feature of bicoherence function is that it is bounded between 0 and 1. There are also other normalization methods but they are not popular because their properties have not been extensively studied (Fackrell, 1996).

#### D. Feature extraction

For the DEAP dataset, the bispectrum computation is applied to each EEG sub-band signal for 12 channels and all available videos (40) and participants (32). The channels selected are FP1, FP2, AF3, AF4, F7, T7, P7, O1, Oz, O2, P8, CP6, T8, F8 and Cz, that are located in the fronal lobe and the peripheral of the brain. EEG channel selection can be treated as a feature selection problem. However, unlike usual feature selection, it is essential to treat all features coming from a channel together, because each EEG channel may contain more than one feature. In EEG emotion recognition, EEG channel selection has been proved to be the main

factor affecting the performance of emotion recognition with the deepening of research. The main task of EEG channel selection is to select a part of electrodes from all electrodes to reduce the computational cost and improve the accuracy rate of emotion recognition. Fig.8 shows the magnitude of the bispectrum in of the EEG signals rhythms corresponding to four emotions classes for Fp1 channel.

The direct method was used in this study to estimate bispectrum using the bispecd function of the MATLAB Higher Order Statistics Toolbox (HOSA). The number of points used to form each fast Fourier transform (NFFT) was 1024. The bispectrum features were extracted from data by using 50% overlap with Rao-Gabr optimal window of length 5. The preprocessed time domain EEG data were segmented into eight seconds length for every channel. Each data segment is also known as an epoch, and contains 1024 data. Four types of EEG frequency sub-bands were used for analysis, namely the theta (4-8) alpha (8-16) Hz, beta (16-32) Hz and gamma (32-64) Hz bands.

Bispectrum features were computed from the non-redundant region  $\Omega$  (Fig. 4) of bispectrum. The features extracted from each trial (32x40xnumber-of-selected-channels (15)) and for each sub-band were based on the magnitude of the bispectrum and these are: mean (H1), standard deviation (H2), maximum value (H3), skewness (H4), kurtosis (H5), differential entropy (H6), euclidean distance between coupling frequency pairs of emotional state and baseline (H8), number of peaks having a counting threshold higher than the 80% of the maximum peak observed (H9), coupling frequency pairs coordinates  $(f_1, f_2)$  (H10), average bispectrum per label across all videos and participants (H11). It should be noted that the number of videos per emotional state wasn't balanced: 439 (HVHA), 269 (HVL A), 298 (LVHA), 274 (LVLA).

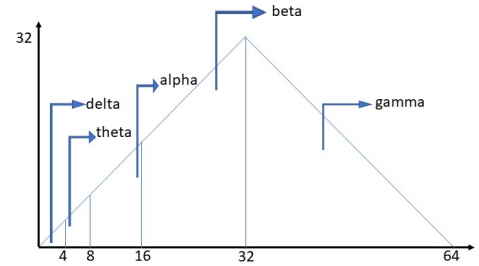


Fig. 4: Non redundant region divided to sub-bands

The mean of the magnitude of the bispectrum (MMOB) is defined as:

$$H1 = \frac{1}{L} \sum_{\Omega} |B(f_1, f_2)| \quad (9)$$

where  $L$  is the number of bispectrum matrix.

The standard deviation of the magnitude of the bispectrum matrix is computed as:

$$H2 = \sqrt{\frac{1}{L} \sum_{\Omega} (|B(f_1, f_2)| - H1)^2} \quad (10)$$

The standard deviation is also an indicator of the peakiness (widely distributed, narrow distributed - sharp).

The differential entropy for a random variable  $X$  is calculated as [17], assuming Gaussian distribution for EEG probability density function:

$$H6 = h(X) = - \int_{-\infty}^{\infty} \frac{1}{2\sigma^2} \exp\left(-\frac{(x-\mu)^2}{2\sigma^2}\right) \log \frac{1}{\sqrt{2\pi\sigma^2}} \exp\left(-\frac{(x-\mu)^2}{2\sigma^2}\right) dx = \frac{1}{2} \log(2e\pi\sigma^2) \quad (11)$$

For the features H8, H9, H10, there is the common challenge of efficiently detecting the significant peaks neglecting the noisy ones as a source of artifacts. In this study, a naive algorithm for peak detection is implemented collecting the maximum values that are higher than 80% of the maximum value of the bispectrum matrix, while neglecting the ones that are very close to each other (assumed as artifacts from the main coupling frequency). For the neglecting stage, a window patch is applied per sorted values that passed the threshold, centering the value of the tested peak and clearing the ones within the patch. In the literature, for the task of peak detection, image processing techniques for edge detection have been utilized e.g. Laplace operator [18], that could potential provide better results.

For features H1-10, to ensure reliability and statistical power, outliers have been removed using the Hampel filter. Normalization techniques for these features have also been applied. Two main techniques have been used: a) divide the feature calculated for the emotional state with the equivalent one of the extracted baseline signal:

$$\frac{H_{i,emot. state}}{H_{i,baseline}} \quad (12)$$

where  $H_i$  is the  $i^{th}$  feature for  $i = 1 - 6$

and b) calculate the feature based on a normalized signal given by:

$$X_{emot. state}(t) = X_{emot. state}(t) - \text{mean}(X_{baseline}(t)) \quad (13)$$

The mean values of the aforementioned features can be found in Table I.

### E. Cepstral analysis

In order to enrich the feature representation making use of EEG periodic patterns, this paper applies a preliminary research based on cepstrum and period detection that can be further expanded using cepstral coefficients. An effort to uncouple interesting properties using High Order Statistics for cepstral analysis has also been made using bicepstrum. The function bicepsf is utilized for this task trying to deduce the impulse response.

The cepstrum of a signal is defined as the inverse Fourier transform of logarithmic magnitude of the spectrum [19], [20], [21]. The real cepstrum of signal  $x(t)$  is calculated as follows:

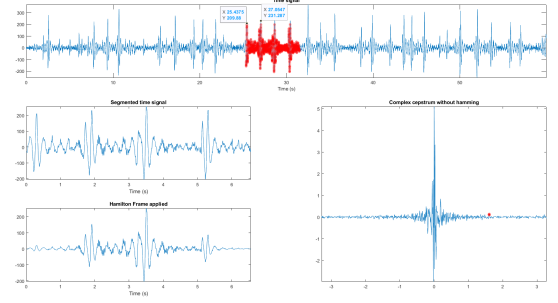


Fig. 5: The fundamental quefrency is the period of the segmented EEG signal

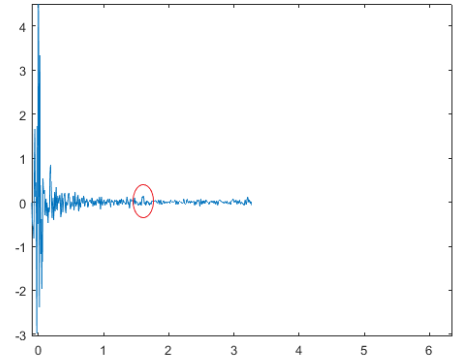


Fig. 6: A zoomed in version of the complex cepstrum

$$c(n) = \frac{1}{2\pi} \int_{-\pi}^{\pi} \log|X(\omega)| e^{i\omega n} d\omega \quad (14)$$

Cepstrum is well-known for speech applications. It can be used for detecting the fundamental pitch period and extracting the source and the impulse response assuming convoluted output.

In the Fig. 5 and 6, we can observe the ability of the cepstrum to detect the fundamental period of a segmented EEG periodic pattern. A more thorough analysis using cepstrum for period detection could unfold a distinguished feature to classify emotion regions based on the value of the periodic patterns observed for time series with different emotional labels. EEG periodicity within a timeseries vary but this variation could be dependent of subject's emotions. These periodic patterns in order to be meaningful should be filtered by blinking artifacts. The depicted timeseries in Fig.5 due to its behaviour and period may be subject of blinking although it is extracted by the preprocessed data.

Unconvenient phase wrapping methods used for cepstrum analysis, lead us to transfer the concept of cepstrum to High Order Statistics with the so called bicepstrum. It can compute the cepstral coefficients directly from the third order cumulants without any phase unwrapping method. In our study we applied bicepstrum to EEG signals with the following basic idea.

A very simple macroscopic model of the EEG signal consists of the brain's impulse response (IR)  $h$ , and white noise as input based on the neural mass models [22].



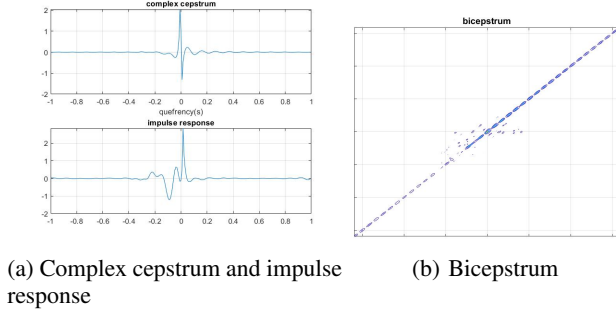


Fig. 7

Thus, bicepstrum can be used to calculate the system's IR [23]. Bicepstrum along the axis and the line  $y=x$  gives the cepstral coefficients that contain the minimum and maximum phase information of the IR and is zero elsewhere (Fig. 7). For calculation of the bicepstrum and the system's IR the function `bicepsf` was used from HOSA Matlab toolbox. This function estimates the impulse response of the EEG using the bicepstrum Fast Fourier Transform (FFT) method without requiring phase unwarping [24].

#### IV. HEMISPHERIC ASSYMETRY FOR EEG EMOTION RECOGNITION

In the past years, many researchers have attempted to utilize the difference between left and right hemispheres as prior knowledge to extract features or develop models, effectively enhancing the performance of EEG emotion recognition. For example, Hinrikus et al. [25] used EEG spectral asymmetry index for depression detection. Lin et al. [9] investigated the relationships between emotional states and brain activities, and extracted PSD, differential asymmetry power, and rational asymmetry power as features. Motivated by their previous findings of critical brain areas for emotion recognition, Zheng et al. [26] selected six symmetrical temporal lobe electrodes as the critical channels and propose a network called Emotion-Meter to model EEG emotional signal. Li et al. [27] proposed a novel neural network called BiDANN that separately extracted two brain hemispheric features and achieved the state-of-the-art classification performance. The above literature demonstrates that some researchers have realized the significance of the difference between the left and right hemispheres for EEG emotion recognition.

A feature relative to hemispheric asymmetry, that haven't been used for this study, but we want to investigate it in future studies is the differential asymmetry of DE features, DASM [17]. DE features should be computed for two groups of channels, left and right hemisphere and the DASM feature is calculated as:

$$DASM = DE(X_{left}) - DE(X_{right}) \quad (15)$$

#### V. RESULTS

The average magnitude of the bispectrum across all participant and videos per emotional label (439:HVHA, 269:HVLA,

298:LVHA, 274 :LVLA) for channel Fp1, DEAP dataset is depicted in Figs 8-11 for each sub-band.

The average values of the selected features for Fp1 and Fp2 electrodes, DEAP dataset are shown in Table 1. The value in the parenthesis includes outliers. The labels 'Div' and 'Signal' are referred to the two normalization methods explained in (12) and (13).

#### VI. CONCLUSIONS

The importance of emotion assessment stems from the need to seek information on the severity of emotional impairment symptoms. Therefore, an accurate emotion assessment approach is required to identify the symptoms of mood disorders in stroke patients. This work proposed the use of the bispectrum feature to classify the discrete emotions (anger, disgust, fear, happiness, sadness and surprise). This study aims to develop an accurate emotion identification method, which can be used to recognize the current emotional state of stroke patients during diagnosis.

In this work, the bispectrum reveals the presence of QPC in the EEG signals and exhibits different QPC relations in each emotional state. This difference in the harmonic components and peaks were shown in the bispectrum contour plots arising from the nonlinear interactions between neuronal populations in each emotional state. In this study, the proposed method of emotion classification by using the bispectrum feature has shown that the effort of finding distinguished factors for emotion classification focusing per channel and per feature isn't enough to decouple the hidden pattern of emotion recognition. In future work we will construct data sets containing multiple instances of signals that originate from one individual, with the expected effect of achieving much better classification accuracy. Another idea is to pinpoint the emotional state within the 60s timeseries by dividing the signal to 3 seconds segments and to compare them with the 3 seconds baseline.

Also, signals corresponding to the same emotion produced by different people are very different. Literature suggests that channels associated to the frontal lobe carry most useful information with respect to the emotion recognition task

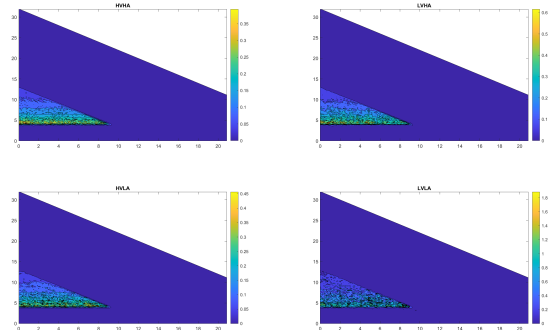


Fig. 8: Gamma (32-64 Hz)

#### VII. IMPLEMENTATION

The code for the given analysis can be found at this public repository: <https://github.com/chrysatbr/EEG-Emotion-Recognition>.

|                      |        | HVHA          |               | HVLA          |               | LVHA          |               | LVLA          |               |
|----------------------|--------|---------------|---------------|---------------|---------------|---------------|---------------|---------------|---------------|
|                      |        | Fp1           | Fp2           | Fp1           | Fp2           | Fp1           | Fp2           | Fp1           | Fp2           |
| Mean                 | Raw    | 0.011 (0.14)  | 0.017 (0.68)  | 0.007 (0.11)  | 0.02 (0.68)   | 0.009 (0.16)  | 0.011 (0.91)  | 0.013 (0.26)  | 0.019 (1.33)  |
|                      | Div    | 0.28 (0.56)   | 0.30 (0.76)   | 0.25 (0.55)   | 0.27 (0.77)   | 0.27 (0.58)   | 0.27 (0.58)   | 0.22 (0.57)   | 0.25 (0.75)   |
|                      | Signal | 0.011 (0.14)  | 0.017 (0.68)  | 0.007 (0.11)  | 0.02 (0.68)   | 0.0089 (0.15) | 0.011 (0.91)  | 0.013 (0.26)  | 0.019 (1.33)  |
| Max                  | Raw    | 1.84 (79.97)  | 2.66 (291)    | 0.85 (50.68)  | 4.155 (272)   | 0.94 (82.44)  | 2.14 (316)    | 2.50 (97.27)  | 4.49 (454)    |
|                      | Div    | 0.27 (2.17)   | 0.27 (2.18)   | 0.28 (2.13)   | 0.28 (2.13)   | 0.24 (1.66)   | 0.24 (1.66)   | 0.21 (4.49)   | 0.21 (4.49)   |
|                      | Signal | 1.84 (79.97)  | 2.66 (291)    | 0.85 (50.58)  | 4.15 (272)    | 0.94 (82.44)  | 2.14 (316)    | 2.57 (97.27)  | 4.49 (454)    |
| Std                  | Raw    | 0.03 (1.15)   | 0.05 (4.29)   | 0.021 (0.77)  | 0.07 (4.45)   | 0.024 (1.18)  | 0.04 (4.71)   | 0.05 (1.54)   | 0.07 (7.63)   |
|                      | Div    | 0.27 (0.88)   | 0.30 (1.41)   | 0.24 (0.99)   | 0.29 (1.47)   | 0.25 (0.39)   | 0.25 (1.37)   | 0.22 (1.35)   | 0.23 (1.96)   |
|                      | Signal | 0.03 (1.15)   | 0.56 (4.29)   | 0.02 (0.77)   | 0.07 (4.45)   | 0.024 (1.18)  | 0.04 (4.71)   | 0.05 (1.54)   | 0.07 (7.63)   |
| Skewness             | Raw    | 16.22 (16.32) | 18 (18)       | 14.94 (15.5)  | 19.21 (19.38) | 14.38 (14.59) | 18.41 (18.65) | 17.66 (18.07) | 19.81 (20.09) |
|                      | Div    | 0.98 (1.15)   | 0.99 (1.21)   | 0.94 (1.16)   | 0.99 (1.21)   | 0.94 (1.13)   | 0.95 (1.21)   | 0.97 (1.2)    | 0.98 (1.22)   |
|                      | Signal | 16.22 (16.30) | 18 (18)       | 14.94 (15.5)  | 19.21 (19.38) | 14.38 (14.59) | 18.41 (18.6)  | 17.68 (18.07) | 19.8 (20)     |
| Kurtosis             | Raw    | 473 (573)     | 581 (655)     | 362 (539)     | 631 (730)     | 372 (477)     | 607 (694)     | 546 (701)     | 680 (812)     |
|                      | Div    | 0.88 (1.92)   | 0.88 (2.10)   | 0.80 (2.2)    | 0.96 (2.04)   | 0.87 (1.84)   | 0.88 (2.04)   | 0.95 (2.11)   | 1.007 (2.24)  |
|                      | Signal | 16.22 (16.3)  | 18 (18)       | 14.94 (15.50) | 19.21 (19.38) | 14.38 (14.59) | 18.4 (18.6)   | 17.66 (18.07) | 19.81 (20)    |
| Differential Entropy | Raw    | -1.3 (-1.3)   | -0.6 (-0.6)   | -1.8 (-1.8)   | -0.57 (-0.57) | 1.88 (-1.69)  | -0.48(-0.48)  | -1.14 (-1.14) | -0.37 (0.37)  |
|                      | Div    | 0.79 (1.31)   | 0.64 (0.22)   | 0.96 (0.77)   | 0.58 (-0.12)  | 0.87 (-1.05)  | 0.71 (0.0084) | 0.75 (0.62)   | 0.76 (2.72)   |
|                      | Signal | -1.3 (-1.3)   | -0.62 (-0.62) | -1.8 (-1.79)  | -0.57 (-0.57) | -1.88 (1.69)  | -0.48 (-0.48) | -1.14 (-1.14) | -0.37 (-0.37) |

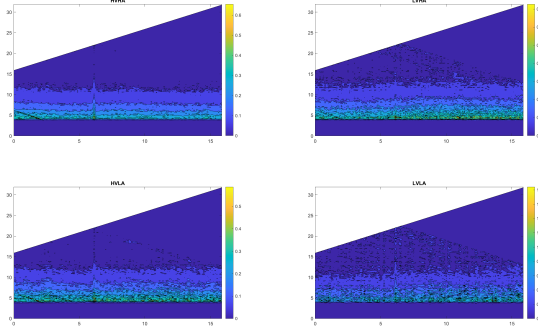
TABLE I: Average feature values per emotional label for the non-redundant region  $\Omega$ 

Fig. 9: Beta (16-32 Hz)

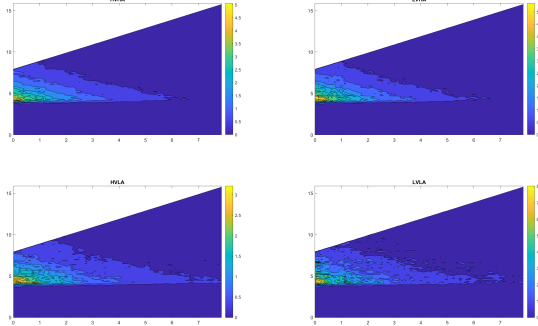


Fig. 10: Alpha (8-16 Hz)

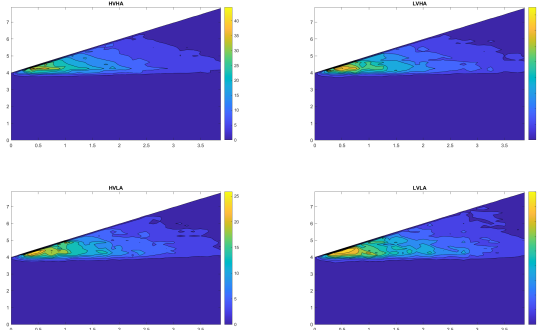


Fig. 11: Theta (4-8 Hz)

## REFERENCES

- [1] S. Koelstra, C. Muhl, M. Soleymani, J.-S. Lee, A. Yazdani, T. Ebrahimi, T. Pun, A. Nijholt, and I. Patras, "Deap: A database for emotion analysis; using physiological signals," *IEEE transactions on affective computing*, vol. 3, no. 1, pp. 18–31, 2011.
- [2] W.-L. Zheng and B.-L. Lu, "Investigating critical frequency bands and channels for eeg-based emotion recognition with deep neural networks," *IEEE Transactions on Autonomous Mental Development*, vol. 7, no. 3, pp. 162–175, 2015.
- [3] S. Mallat, *A wavelet tour of signal processing*. Elsevier, 1999.
- [4] C. K. Chui, *Wavelets: a tutorial in theory and applications*. Academic Press Professional, Inc., 1993.
- [5] M. Murugappan, N. Ramachandran, Y. Sazali *et al.*, "Classification of human emotion from eeg using discrete wavelet transform," *Journal of biomedical science and engineering*, vol. 3, no. 04, p. 390, 2010.
- [6] C. L. Nikias, "Higher-order spectral analysis," in *Proceedings of the 15th Annual International Conference of the IEEE Engineering in Medicine and Biology Society*. IEEE, 1993, pp. 319–319.
- [7] C. L. Nikias and M. R. Raghuveer, "Bispectrum estimation: A digital signal processing framework," *Proceedings of the IEEE*, vol. 75, no. 7, pp. 869–891, 1987.
- [8] C. L. Nikias and J. M. Mendel, "Signal processing with higher-order spectra," *IEEE Signal processing magazine*, vol. 10, no. 3, pp. 10–37, 1993.
- [9] Y.-P. Lin, C.-H. Wang, T.-P. Jung, T.-L. Wu, S.-K. Jeng, J.-R. Duann, and J.-H. Chen, "Eeg-based emotion recognition in music listening," *IEEE Transactions on Biomedical Engineering*, vol. 57, no. 7, pp. 1798–1806, 2010.
- [10] R. Sharma, P. Sircar, R. Pachori, S. V. Bhandary, and U. R. Acharya, "Automated glaucoma detection using center slice of higher order statistics," *Journal of Mechanics in Medicine and Biology*, vol. 19, no. 01, p. 1940011, 2019.
- [11] S. A. Hosseini, M. A. Khalilzadeh, M. B. Naghibi-Sistani, and V. Niazmand, "Higher order spectra analysis of eeg signals in emotional stress states," in *2010 Second international conference on information technology and computer science*. IEEE, 2010, pp. 60–63.
- [12] R. Sharma, P. Sircar, and R. B. Pachori, "Computer-aided diagnosis of epilepsy using bispectrum of eeg signals," in *Application of Biomedical Engineering in Neuroscience*. Springer, 2019, pp. 197–220.
- [13] J. Fonoliosa and C. Nikias, "Wigner higher order moment spectra: definition, properties, computation and application to transient signal analysis," *IEEE Transactions on Signal Processing*, vol. 41, no. 1, p. 245, 1993.
- [14] R. Sharma, R. B. Pachori, and P. Sircar, "Automated emotion recognition based on higher order statistics and deep learning algorithm," *Biomedical Signal Processing and Control*, vol. 58, p. 101867, 2020.
- [15] P. Venkatakrisnan, R. Sukanesh, and S. Sangeetha, "Detection of quadratic phase coupling from human eeg signals using higher order statistics and spectra," *Signal, Image and Video Processing*, vol. 5, no. 2, pp. 217–229, 2011.
- [16] W. Kiciński and A. Szczepański, "Quadratic phase coupling phenomenon and its properties," *Hydroacoustics*, vol. 7, pp. 97–106, 2004.

- [17] N. M. Wasekar, C. J. Gaikwad, and M. M. Dongre, "Eeg signal analysis and emotion classification using bispectrum," in *Computational Methods and Data Engineering*. Springer, 2021, pp. 385–395.
- [18] S. Bartz, C. Andreou, and G. Nolte, "Beyond pairwise interactions: the totally antisymmetric part of the bispectrum as coupling measure of at least three interacting sources," *Frontiers in Neuroinformatics*, vol. 14, p. 48, 2020.
- [19] K. Van Loon, F. Guiza, G. Meyfroidt, J.-M. Aerts, J. Ramon, H. Blockeel, M. Bruynooghe, G. Van den Berghe, and D. Berckmans, "Prediction of clinical conditions after coronary bypass surgery using dynamic data analysis," *Journal of medical systems*, vol. 34, no. 3, pp. 229–239, 2010.
- [20] D. G. Childers, D. P. Skinner, and R. C. Kemerait, "The cepstrum: A guide to processing," *Proceedings of the IEEE*, vol. 65, no. 10, pp. 1428–1443, 1977.
- [21] N. Sho'ouri, "Cepstral analysis of eeg during visual perception and mental imagery reveals the influence of artistic expertise," *Journal of Medical Signals and Sensors*, vol. 6, pp. 203–217, 10 2016.
- [22] S. Shahid and J. Walker, "Cepstrum of bispectrum—a new approach to blind system reconstruction," *Signal Processing*, vol. 88, no. 1, pp. 19–32, 2008.
- [23] D. Cosandier-Rimélé, J.-M. Badier, P. Chauvel, and F. Wendling, "Modeling and interpretation of scalp-eeg and depth-eeg signals during interictal activity," in *2007 29th Annual International Conference of the IEEE Engineering in Medicine and Biology Society*. IEEE, 2007, pp. 4277–4280.
- [24] R. Pan and C. L. Nikias, "The complex cepstrum of higher order cumulants and nonminimum phase system identification," *IEEE transactions on acoustics, speech, and signal processing*, vol. 36, no. 2, pp. 186–205, 1988.
- [25] H. Hinrikus, A. Suhhova, M. Bachmann, K. Aadamssoo, Ü. Vöhma, J. Lass, and V. Tuulik, "Electroencephalographic spectral asymmetry index for detection of depression," *Medical & biological engineering & computing*, vol. 47, no. 12, pp. 1291–1299, 2009.
- [26] W.-L. Zheng, W. Liu, Y. Lu, B.-L. Lu, and A. Cichocki, "Emotionmeter: A multimodal framework for recognizing human emotions," *IEEE Transactions on Cybernetics*, vol. 49, no. 3, pp. 1110–1122, 2019.
- [27] Y. Li, W. Zheng, Y. Zong, Z. Cui, T. Zhang, and X. Zhou, "A bi-hemisphere domain adversarial neural network model for eeg emotion recognition," *IEEE Transactions on Affective Computing*, 2018.